AIP | Review of Scientific Instruments

Picosecond timeresolved circular dichroism spectroscopy: experimental details and applications

Xiaoliang Xie and John D. Simon

Citation: Review of Scientific Instruments **60**, 2614 (1989); doi: 10.1063/1.1140681
View online: http://dx.doi.org/10.1063/1.1140681
View Table of Contents: http://scitation.aip.org/content/aip/journal/rsi/60/8?ver=pdfcov
Published by the AIP Publishing

Picosecond time-resolved circular dichroism spectroscopy: experimental details and applications

Xiaoliang Xie and John D. Simon

Department of Chemistry B-041, University of California, San Diego, La Jolla, California 92093

(Received 14 February 1989; accepted for publication 27 March 1989)

An experimental apparatus for measuring time-resolved circular dichroism (CD) with picosecond resolution is described. The time resolution of the device is determined by the laser pulse width, not the modulation frequency of an electro-optic or piezo-optic crystal as is the case for commercial CD spectrometers. The time-dependent CD signal can be monitored over the wavelength range from 280 to 850 nm. The data from single wavelength studies can be pieced together to generate time dependent spectra. The experimental approach is compared to previous time-resolved CD techniques which, for technical reasons, have been limited to, at most, nanosecond resolution. The picosecond apparatus is shown to be free of many of the polarization artifacts present in these previous devices. The utility of this technique is demonstrated by examining result on the time dependent near-UV CD of myoglobin following the photoelimination of coordinated CO from carbonmonoxymyoglobin.

INTRODUCTION

Due to the tremendous theoretical and instrumental work which has occurred in the past several decades, circular dichroism (CD) spectroscopy has matured into a powerful and popular spectroscopic tool for probing the conformation of molecules in solution.[1] In particular, CD spectroscopy has become one of the most prominent techniques for studying conformational properties of biochemical systems. CD is one of many techniques which are currently being used to probe the structure of proteins. Data on protein structure primarily comes from x-ray diffraction data of single crystals. These experiments provide detailed information on the locations of all of the atoms in the protein, and analyses of the mean square deviations of the atomic coordinates can be used to obtain information on protein conformational motions.[2] However, such an averaged measurement is not elucidative about the time scales of the conformational motions and is not necessarily in accord with the molecular structure in solution where biomolecules are believed to be more mobile. Significant differences between the protein structure in solution and in a single crystal can be imagined. In the crystal, motions of side-chains and large scale "vibrational" fluctuations would be eliminated. In solution, these motions could play a deterministic role in the conformational changes which occur as the protein exhibits its biological behavior. Clearly, techniques in addition to x-ray crystallography are needed if we are to understand the underlying relationships between protein structure/dynamics and its function.

NMR and fluorescence depolarization spectroscopy are currently the most widely used techniques for examining conformation dynamics in macromolecules.[3,4] While slow conformational exchange can be directly measured by NMR, fast conformational motion with the time scale ranging from microseconds to picoseconds can be deduced from relaxation measurements. These conformational changes are usually local, within at most 5 A from the nuclei being probed.

The measurement of the fluorescence anisotropy[4] of an intrinsic fluorophore (i.e., tryptophan in protein) or extrinsic probe (i.e., a dye intercalated in DNA) can provide information about (1) the local conformational motion near the fluorophore, and (2) the overall tumbling motion of the biomolecule. Recently, this experimental approach has been extended to examine motions in the subpicosecond time domain.[5] Other forms of picosecond time-resolved spectroscopy (e.g., absorption, transient grating, Raman) have also been used to examine biochemical systems.[6] While the time dependent Raman spectra might reflect local structural changes (which might tie to global rearrangements), information about protein relaxation cannot generally be obtained from studies on the temporal dependence of the intensity or band shape of electronic transitions.

On the other hand, time-resolved CD would enable one to directly monitor molecular motions. Since CD is uniquely sensitive to molecular conformation, time-resolved studies could be used to characterize conformational intermediates, providing data which is complimentary to that obtained from the above-mentioned transient spectroscopies. Experimental devices for measuring time-resolved CD spectra have been reported in the last two decades.[7,8] Using these apparatuses, some results of biological interest[9] have appeared. However, due to technical reasons, the time resolution of such approaches has been limited to nanosecond or slower time scales.

In this article, we report a new approach for the collection of time-resolved CD data. The experimental design is not a simple extension of previous techniques, but represents a novel approach combining high power, high-repetition-rate picosecond lasers with a newly developed electronic detection and electro-optic modulation scheme. There are two significant advances afforded by our experimental design.

 0034-6748/89/082614-14$01.30

First of all, the time resolution is only limited by the laser pulse width. Although we demonstrate a 80-ps time resolution in this article, with currently available ultrafast laser systems, subpicosecond resolution can be easily achieved. The second advantage is that the experimental design is essentially free of the effects of pump-induced linear birefringence and linear dichroism; these polarization artifacts have plagued previous experimental approaches. An application of picosecond time-resolved circular dichroism spectroscopy to biological process is discussed in the final section of the article. The time dependence of the change in the near-UV CD signal of myoglobin (Mb) following photoelimination of CO from carbonmonoxymyoglobin (MbCO) is examined.

I. BACKGROUND

A. Connection between circular dichroism and molecular conformation

Optical activity of a chiral molecule is characterized by properties known as circular dichroism (CD) and circular birefringence. CD is the differential absorption of left and right circularly polarized light and is quantified by the difference between the extinction coefficients with respect to these two polarizations: $\Delta\epsilon = \epsilon_L - \epsilon_R$. This difference only occurs at wavelengths where there is an absorption and the value of the CD signal can be either positive, negative, or zero. On the other hand, circular birefringence is characterized by a difference of the index of refraction with respect to left and right circularly polarized light, $n_l - n_r$. The magnitude of the circular birefringence can be obtained from an optical rotation measurement in which the polarization axis of a linear polarized light is rotated by the chiral sample. The optical rotation as a function of wavelength is called the optical rotatory dispersion (ORD). CD and ORD spectra are not independent. They obey the general relationship between absorption and dispersion, the Kronig-Kramers transforms.[10] In practice, circular birefringence occurs at virtually all wavelengths, resulting in a featureless ORD spectrum. CD spectra, on the other hand, usually have sharp, well-defined peaks. As a result, CD spectroscopy has been the favored tool for studying chemical and biological systems, despite the ease of ORD measurements.

One significant advantage of CD spectroscopy is that the data can be related to structural features of the molecule being studied. In particular, the connection between CD and molecular conformation has been mathematically described in terms of a quantum mechanical quantity called the rotational strength. The rotational strength, R_{0a}, of a transition between two stationary states, $\Psi_0 \rightarrow \Psi_a$, is represented by the scalar product of the electric dipole, μ_e^{0a}, and the magnetic dipole, μ_m^{0a}, transition moments.[11]

$$R_{0a} = \mathrm{Im}\left(\int \Psi_0 \hat{\mu}_e \Psi_a \, d\tau\right)\left(\int \Psi_0 \hat{\mu}_m \Psi_a \, d\tau\right). \qquad (1)$$

In the above expression, Im signifies that the imaginary part of the integral is evaluated. This results in the rotational strength being a real quantity, as the magnetic dipole operator, $\hat{\mu}_m = (e/2mc)(\hat{\mathbf{r}} \times \hat{\mathbf{p}})$, is purely imaginary. A group theoretical analysis of the two integrals in Eq. (1) indicates that a nonzero rotation strength exists for molecules belonging to C_n and D_n groups. Thus, optical activity necessitates a chiral molecular structure. A quantum mechanical formulation presented by Rosenfeld in 1928 (Ref. 12) revealed the connection between R_{0a} and CD ($\Delta\epsilon = \epsilon_l - \epsilon_r$).

$$R_{0a} = \frac{3hc10^3 \ln 10}{32\pi^3 N_A} \int [\Delta\epsilon(\lambda)]/\lambda \, d\lambda \, . \qquad (2)$$

In the above expression, h is Planck's constant, c is the speed of light, and N_A is Avogadro's number. The integral in Eq. (2) is evaluated over the wavelength range corresponding to the transition from state 0 to state a. In principle, knowledge of the wave functions can lead to a direct calculation of the CD spectrum. This expression implies how structural information is manifested in the CD spectrum.

Circular dichroism is commonly measured in many spectral regions. Infrared techniques are used to measure the CD of vibrational transitions within a given electronic state while ultraviolet/visible (UV-Vis) CD provides information on transitions between different electronic states. For protein studies, UV-Vis CD spectroscopy is commonly used. CD in UV region of the spectrum has been extensively used as a probe for the secondary structures of proteins. While the UV absorption of an α helix, β sheet, or randomly coiled polypeptide are essentially indistinguishable their CD spectra are very different. Using a semiempirical analysis of the UV CD spectrum,[13] one can deduce the relative content of these conformations in the protein. CD in the wavelength region from 250 to 300 nm, commonly called the aromatic range, is usually dominated by the contribution from aromatic side-chains. CD in visible part of the spectrum (350–600 nm) provides information on prosthetic groups, such as metal-porphyrins and retinal. Both experiments and calculations have indicated that CD in the aromatic and visible ranges probe the tertiary and quaternary protein structures. Time-resolved studies throughout these wavelength regions would provide information on the time scales of these type of protein motions.

B. Techniques for measuring steady-state CD spectra

For most chiral molecules, the differential absorption of left and right circular polarized light is very small, $10^{-6} < \Delta\epsilon/\epsilon < 10^{-3}$. This small signal can easily be buried in measurement noise or complicated by various polarization artifacts. Therefore, sensitive detection systems are required. Two approaches are commonly used, one measures ellipticity, the other employs polarization modulation and phase-sensitive detection.

Ellipticity measurements date back to the beginning of this century.[14] This method takes advantage of the fact that a linearly polarized light beam can be viewed as a composition of equal amplitude left and right circularly polarized light. When linear polarized light is passed through an optical active medium, one of the circular components is absorbed more than the other (see Fig. 1 for details) producing an

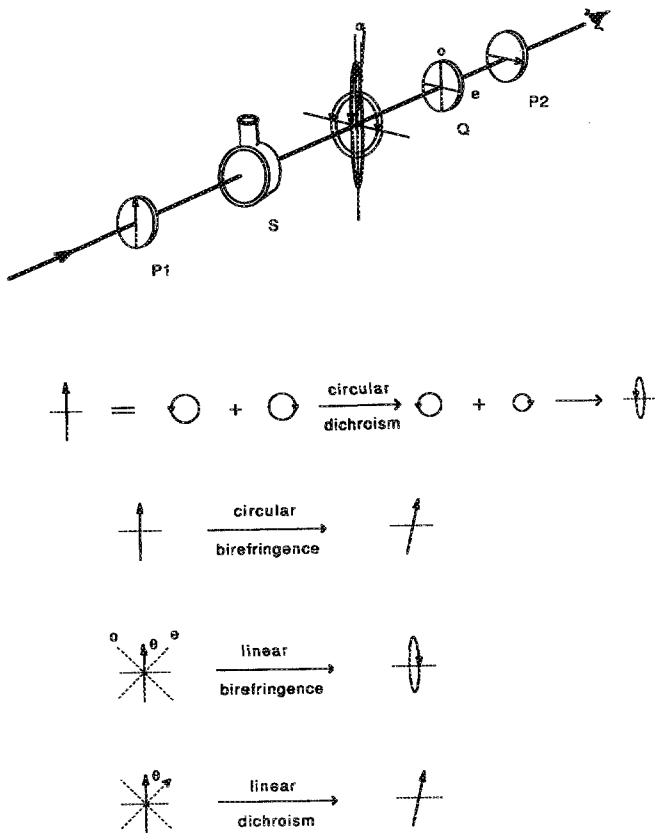

FIG. 1. Schematic of the traditional ellipticity measurement and illustration of the effects of circular birefringence, linear birefringence, and dichroism on the observed signal. The polarizer, $P1$, produces linearly polarized light. This beam is converted to elliptically polarized light after passing through the circularly dichroic sample, S. The quarter wave plate, Q, converts the elliptically polarized light back into a linearly polarized light. The crossed polarizer, $P2$, is rotated until the eye observes the extinction of the transmitted light. The ellipticity, α, is measured by the angle of rotation of $P2$. The bottom diagrams show how circular birefringence, linear birefringence, and dichroism contribute to the observed signal. The horizontal dotted lines represent the polarization axis of the crossed polarizer. Circular birefringence of the optical active sample causes a rotation of the polarization axis (optical rotation). Linear birefringence of the cell can cause a conversion of the linearly polarized light into elliptically polarized light. θ is the angle between the polarization axis of the probe light and the extraordinary axis. Linear dichroism of the cell is usually negligible if the cell is transparent. However, if one were to measure time-resolved CD using linearly polarized light to excite the sample, the effect of the pumped-induced linear dichroism of sample would be a rotation of the polarization axis of the probe light. θ is the angle between the polarization axes of the pump and probe light.

output beam which is elliptically polarized with the major axis parallel to that of the incident linearly polarized light beam. The ellipticity, defined as the arc tangent of the ratio of the minor axis to the major axis of the ellipse, is proportional to $\Delta\epsilon$. Following the sample, a quarter-wave plate, with its fast or slow axis along the polarization direction of the incident beam, is used to convert the elliptical light back into a linearly polarized beam. The resulting polarization direction is rotated with respect to the original polarization axis of the light. A final analyzing polarizer, at first perpendicular to the original polarization direction, is then rotated until the transmission is extinguished. In this way, ellipticity is easily quantified by measuring the angle of rotation of the analyzing polarizer. However, this method has several inherent complications. The optical rotation due to circular birefringence of the chiral sample also causes a rotation of the polarization of the linearly polarized light (see Fig. 1). Although this effect does not change the ellipticity of the probe beam, it rotates the ellipse. Using the detection process described above, this would effect the observed signal, rendering an accurate measure of the CD of the sample difficult. Further complications arise from the linear birefringence of the sample cell. Due to strain in materials such as quartz, the optical cell is often nonisotropic and acts as a phase retarder. As shown in Fig. 1, this would also cause a conversion of the incident light into an elliptically polarized beam, providing an additional component to the measured signal.

Polarization modulation[15] is the basis of present day commercial CD spectrometers. Invented in 1960, it has made the routine collection of CD spectra possible. This technology has been recently reviewed.[16] In general, a monochromatic linearly polarized light beam is passed through an electro-optic (or piezo-optic) modulator in which the light beam is switched between left and right circularly polarized light of equal intensity. This modulated light beam is directed through a sample, and processed by a phase sensitive detector (lock-in amplifier) referenced at the modulation frequency. This approach is not only more sensitive than ellipticity measurements, but is less prone to polarization artifacts. The modulation technique eliminates the need for any analyzing of the polarization of the beam after passing through the sample. As a result, the optical rotation of the sample, circular birefringence, has no effect on the measured signal.

C. Previous approaches for measuring transient CD spectra

Using the polarization modulation detection scheme, stop flow,[7] and flash photolysis[8] CD spectrometers have been developed. The former can be done by modifying the sample cell in a commercial CD spectrometer. The time resolution is microseconds, subject to the limitation of any stop-flow technique. The latter method measures the time profile of the CD signal following a short photoexcitation pulse. This technique requires detectors with fast-time responses. One desires to make a measurement as fast as possible in order to follow transient processes which occur immediately following the photoexcitation. Due to the fact that the highest modulation rate of a piezo-optic device is 50 kHz, the time resolution of a flash photolysis CD experiment had been limited to milliseconds. It was commonly believed that the time resolution of CD spectroscopy was restricted by the polarization modulation frequency.[16]

Recently Kliger and coworkers developed a nanosecond time-resolved CD technique which is a variant of the ellipticity measurement described above.[17–20] In this flash photolysis experiment, a nanosecond laser (with high energy and low repetition rate) is used to excite the sample. Photoinduced CD changes are monitored by measuring the change in ellipticity of a probe beam. In this particular experimental apparatus, a polarizer is used to generate a linearly polarized

probe beam from the output of a high-intensity flash lamp. This light beam is passed through a strained quartz plate which acts as a slight phase retarder. Depending on the orientation of the fast axis of the plate ($+45°$ or $-45°$ with respect to the polarization direction of the beam), the light is converted to highly eccentric left or right elliptically polarized light. When this light passes through a circular dichroic sample, the ellipticity is changed. This change in ellipticity is monitored by passing the light through a second polarizer which is oriented perpendicular to the first. The transmitted light is dispersed by a monochrometer and detected by a PMT, the output of which is digitized by a transient recorder. The output signal is a measure of the magnitude of the minor axis of the elliptically polarized probe beam, which in turn is directly related to the CD of the sample. This approach advanced transient CD measurements by three order of magnitude and has successfully generated kinetics and spectra of transients on the nanosecond time scale.

However, this technique is subject to all the difficulties associated with the traditional ellipticity measurement discussed above. While the linear birefringence of the sample cell is invariant and can be removed by baseline subtraction of a blank experiment, the circular birefringence of the sample is an inherent complication. A Jones matrix calculation[18] for the myoglobin and hemoglobin system suggested that the ORD contribution to the CD signal is negligible in the visible part of the spectrum but becomes important in the UV range. In addition, there are other complications pertinent to this transient experiment. Laser output is usually linearly polarized. It is hard to completely depolarize a laser beam; thus, the photolysis preferentially excites molecules with transition dipole moments parallel to the polarization axis. This leads to both a pump-induced transient linear dichroism and linear birefringence. As in the case of optical activity, these two effects are not independent but are related by the Kronig–Kramers transform. The possible contribution of linear dichroism to the signal measured using the ellipticity method is illustrated in Fig. 1. At certain orientations of the polarization of the excitation beam, the probe beam is expected to rotate due to the time dependent linear dichroism. In addition, the effect of the induced linear birefringence is to make the sample act like a time dependent phase retarder, changing the measured ellipticity. Both effects disappear as molecular rotation randomizes the orientation of the excited state molecules in the sample.

In fact [neglecting the tiny ellipticity (0.01) created by the strained quartz plate], if the polarization axis of the pump beam is at a 45° angle with respect to the crossed polarizers, the optical arrangement of Kliger *et al.* is identical to a technique developed by Shank and Ippen for measuring linear dichroism.[21] Furthermore, through a series of carefully conducted anisotropic absorption experiments, Waldeck *et al.*[22] demonstrated that both linear dichroism and linear birefringence could be observed using the experimental method of Ippen and Shank. The relative contribution of these effects to the observed signal was molecule dependent.

In accord with these predictions, large spike-like signals were observed immediately following photolysis in the nanosecond time-resolved circular dichroism experiments. These signals were attributed to the pump-induced linear birefringence; however, the possible complications from pump-induced linear dichroism were not addressed.[19] By orienting the excitation polarization axis at 90° with respect to the probe and using a Soleil–Babinet compensator in the pump beam, Kliger and coworkers were able to remove complications from the pumped-induced linear birefringence.

A final complication in the time-dependent ellipticity measurements arises from the fluorescence from excited molecules. The two perpendicular high-extinction polarizers attenuate the probe beam intensity by a factor of at least 10^{-4}. However, these elements have little effect on the emission intensity. As a result, under certain conditions (highly emissive molecules) the amplitude of the emission can be larger than the CD signal rendering an accurate measurement impossible.

Although extension of the time-resolved technique of Kliger *et al.* to the picosecond time domain should be possible, several practical complications result from the fact that (1) picosecond light sources are generally much noisier than either flash lamps or nanosecond lasers, and (2) the contributions from pump-induced linear dichroism, linear birefringence, and sample emission to the observed signal would all increase in importance with higher time resolution.

In developing a picosecond time-resolved circular dichroism spectrometer, we have designed an experimental approach which is free of the difficulties described above. In the next section, the technical details of the laser apparatus, the detection system, and the polarization modulator are discussed.

II. INSTRUMENTATION

Our experimental device is based on the following approach. A high repetition rate picosecond laser system (Sec. II A) is used to generate the pump and probe laser pulses. The picosecond probe pulse train is polarization modulated by an electro-optic modulator (Sec. II C) switching sequential pulses between left and right circular polarization. The light is detected using phase sensitive detection (Sec. II B). The time delay between each pump/probe pulse pair is controlled by a computer driven optical delay line, enabling the evolution of the CD signal at a fixed wavelength following photoexcitation to be determined. On the other hand, scanning the dye laser at a fixed time delay between the pump and probe pulses can generate a transient CD spectrum. It is important to stress that the time resolution of this experiment is limited by the laser pulse width.

A. Picosecond laser system

A schematic of the laser system is shown in Fig. 2. A mode-locked, Q-switched and cavity dumped Nd:YAG laser is used to synchronously pump cavity-dumped dye lasers.[23] The oscillator consists of a Quantronix model 116 CW Nd:YAG laser head which is acousto-optically mode locked at 50 MHz (Interaction Corporation model ML-50Q), and acousto-optically Q-switched at repetition rate 1 kHz (Interaction Corporation model AQS-244A). The cav-

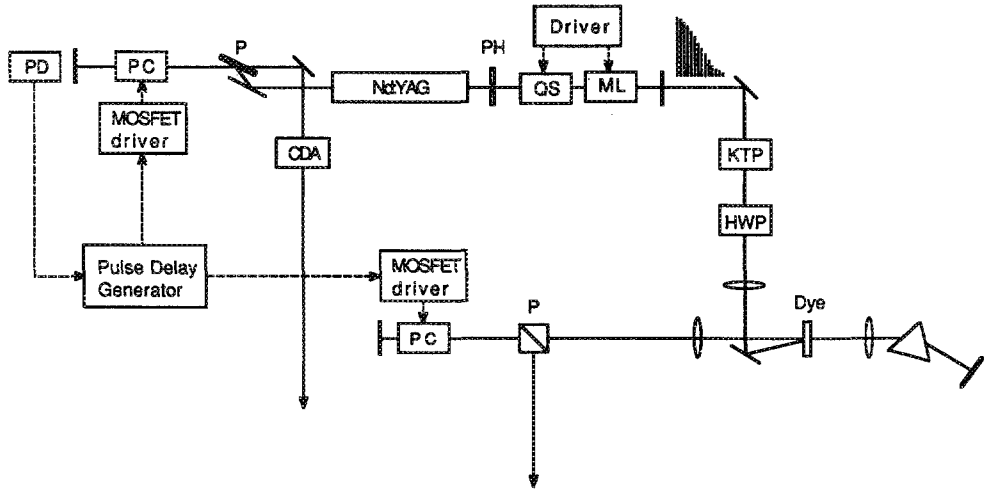

FIG. 2. Block diagram of the mode-locked, Q-switched, cavity dumped Nd:YAG laser and the synchronously pumped dye laser. Abbreviations: PC: Pockels cell, QS: acousto-optic Q-switch, ML: acousto-optic mode-locker, PH: pinhole, HWP: half-wave plate, P: polarizer, PD, fast photodiode. The dye laser is prism tuned providing an output beam with a spectral width of 0.3 mm. For narrower spectral output, a pair of etalons (not shown here) are used.

ity mirrors are a + 100-cm-high reflector and a − 120-cm, 92% reflectivity output coupler. The prelasing level is adjusted by setting the rf power to the Q-switch so that the first prelasing pulse is 400 μs behind the previous Q-switch pulse envelope. Cavity dumping of the oscillator is achieved using a lithium niobate ($LiNbO_4$) transverse Pockels' cell (Interactive Radiation model 204-080), and a dielectric polarizer (CVI). The electro-optic driver is similar in design to that reported by Dlott and coworkers.[24] Using high-voltage MOSFETs to switch the quarter-wave voltage, this device offers superior performance (high repetition rate and increased reliability) over the conventional avalanche transistor chains.

The IR output from the Nd:YAG laser is focused into a $3\times3\times8$-mm^3-piece of KTP (Litton, Airtron) using a 40-cm focal length lens positioned 20 cm in front of the KTP crystal; a 35% conversion to the second harmonic is observed, providing 0.45 mJ of 532-nm light per Q-switch burst. This light is used to synchronously pump the tunable dye laser(s). Dye laser cavity mirrors are flat high reflectors (Virgo). The 1-mm flowing dye cell (Wilmad) sits between a 10-cm and a 20-cm plano-convex lens. The beam waist at the dye cell is approximately 200 μm. Using a prism as the tuning element enables easy wavelength adjustments of the dye laser without walking the laser beam. Prism tuning results in a bandwidth of 0.3 nm. For narrower spectral widths, a pair of etalons are used (Virgo Optics, not shown in Fig. 2). The dye laser is cavity dumped using a polarizer (Newport) KDP Pockels' cell (Quantum Technology) combination. The driver electronics are identical to that used to cavity dump the Nd:YAG oscillator. Using R6G as the gain medium, we obtain 22 μJ/pulse, 20 ps FWHM, and pulse fluctuations of $<5\%$ at 570 nm.

For a cavity-dumped dye laser synchronously pumped by a Q-switched mode-locked Nd:YAG laser, the intracavity dye laser pulse reaches a maximum approximately five round trips after pumping by the maximum intensity pulse of the frequency doubled Nd:YAG Q-switch bell-shaped pulse burst. Once the dye laser pulse is cavity-dumped, the residual pump pulses in the Q-switch envelope are not needed. Cavity dumping the Nd:YAG oscillator immediately following the cavity dumping of the dye laser makes full use of this energy and provides a stable and intense source of picosecond light which is perfectly synchronized to the dye laser. The cavity-dumped IR output has a pulse energy of 0.6 mJ and a pulse width of 80 ps FWHM. Using a 4-cm CD* *A* crystal, we obtain second harmonic pulse energies of $\approx$0.25 mJ. An additional third harmonic mixing crystal generates 50 μJ/pulse at 355 nm. High conversion efficiency for quadrupling can also be obtained by using a temperature tuned 90° phase matching KDP crystal. The fundamental or the harmonics can be used to (1) amplify the dye output, or (2) extend the tuning range of the laser through frequency mixing with the dye laser output, or (3) serve as the excitation beam in the time-resolved experiment.

The timing of the cavity dumping of the Nd:YAG oscillator and the dye laser(s) is controlled by a four-channel digital-delay generator (Stanford Research Systems, model DG 535). This unit is triggered by a fast diode (FND100, E.G.G.) which monitors the IR leakage through the rear mirror of the Nd:YAG oscillator. This timing box is also used to synchronize the driver electronics of the polarization modulator (described in Sec. II C).

The high-repetition rate, stability, and wavelength tunability of this laser system are ideal for the requirements of the picosecond time-resolved circular dichroism experiments. The high-repetition rate allows us to use phase sensitive detection. The fact that the pulse intensity fluctuation is small ($<5\%$) benefits the signal to noise ratio. Using the second harmonic of the Nd:YAG to pump the dye laser generates tunable light throughout the visible and near IR spectral range (560 to 880 nm). Frequency doubling of the dye laser output provides light from 280 to 440 nm with pulse energies of ≈ 1 μJ. Sum frequency mixing of the fundamental of the cavity dumped Nd:YAG and the dye laser pulses (or difference frequency mixing the 4th harmonic of the cavity dumped Nd:YAG pulse and the dye laser output) generates light in the range from 380 to 480 nm. Using β-BBO dou-

bling crystals, the 4th harmonic of the dye laser pulses could open up work in the far-UV where the CD results from peptide absorption. Electro-optic modulators which are transparent over these regions are available (KDP, RDP Pockels' cell). Thus, the laser system can provide probe beams over the entire wavelength range of interest in biochemical systems. In conventional CD measurement, one often requires high intensity lamps for the probe light source in order to obtain measurable CD signals. Using the high-peak power inherent to picosecond (or shorter) laser pulses, a weak probe beam with $<0.1\ \mu J$/pulse is sufficient. Using this approach, probing the time evolution of the CD signal at a fixed wavelength is relatively easy, comparable to conventional pump-probe picosecond experiments. When taking a transient CD spectrum in the wavelength region where nonlinear frequency mixing is needed to generate the probe beam, intracavity etalons must be used to limit the bandwidth of the dye laser. When scanning such a dye laser, one has to compensate for both the walking of the laser beam caused by rotation of the fixed air-gap etalon and the angle tuning of the nonlinear doubling (or mixing) crystal.

In addition to the weak probe beam, the laser system also needs to provide an intense pump beam for excitation. The pump beam can be generated from either the cavity dumped Nd:YAG laser pulse (harmonics at 532, 355, and 266 nm), or from a second synchronously pumped dye laser. We have previously demonstrated[23] that the output from a synchronously pumped dye laser can be amplified to >30 μJ/pulse using the second harmonic of cavity dumped Nd:YAG output to pump a single 1-cm amplifier cell. Using both pump and probe beams from two dye lasers results in our current upper limit of temporal resolution, 20 ps, for the transient CD experiment. If harmonics of the cavity dumped YAG pulse are used as the pump beam, the time resolution decreases to ≈ 80 ps.

It should be pointed out that our picosecond time-resolved circular dichroism technique could be used with any high repetition rate ultrafast laser systems. Regenerative amplified systems[25] as well as copper vapor amplified systems[26] can provide tens of femtosecond pulses at kHz repetition rate. Although these amplified pulses are not tunable, they can be used to generate a white light continuum from 400 to 1000 nm from which the probe wavelength can be selected using narrow band interference filters. If one used these laser systems for time-resolve CD experiments, the only concern would be the group velocity dispersion of the short pulse caused by the long path length of the electro-optic modulator. However, there is no reason why the approach described in this article cannot be extended into the subpicosecond time domain.

B. Detection of the CD signal

A schematic of detecting system is shown in Fig. 3. A well-collimated probe beam is passed through an electro-optic modulator the design of which will be described in detail in the next section. Pulses in the 1-kHz train are sequentially switched to generate alternating left and right circularly polarized laser pulses. The resulting modulation frequency is 500 Hz. This modulated beam is focused by a 25-cm focal length lens into a 2-mm rectangular quartz flow cell (Wilmad). The focal spot is ≈ 0.4 mm in diameter, smaller than that of pump beam, ≈ 0.6 mm. The flow rate of the sample is sufficient that each pump pulse excites fresh sample, reducing the effects of both thermal lensing in the sample and the photolysis of photoproducts. After passing through the sample the probe beam is recollimated by another 25-cm focal length lens and detected by a rf shielded photomultiplier (RCA, model 1P28). The probe beam is attenuated by neutral density filters to ensure a linear intensity response. The PMT is mounted on a translation stage so that the laser beam can be sent to the quietest and most sensitive spot on the photocathode. The signal is amplified by a broad band (DC to 250 MHz) $\times 10$ preamplifier (LeCroy model VV100BTB). A schematic representation of the detected 1-kHz pulse train is shown in Fig. 4; each pulse has a width of ≈ 5 ns and a peak voltage of ≈ 2 V when terminated with a 50-Ω resistor. The circular dichroism of the sample results in a $<0.1\%$ pulse amplitude modulation at 500 Hz; it is this signal that we need to extract. However, this small signal is buried in the overwhelming laser energy fluctuation ($\approx 5\%$). This problem underlies the challenge for picose-

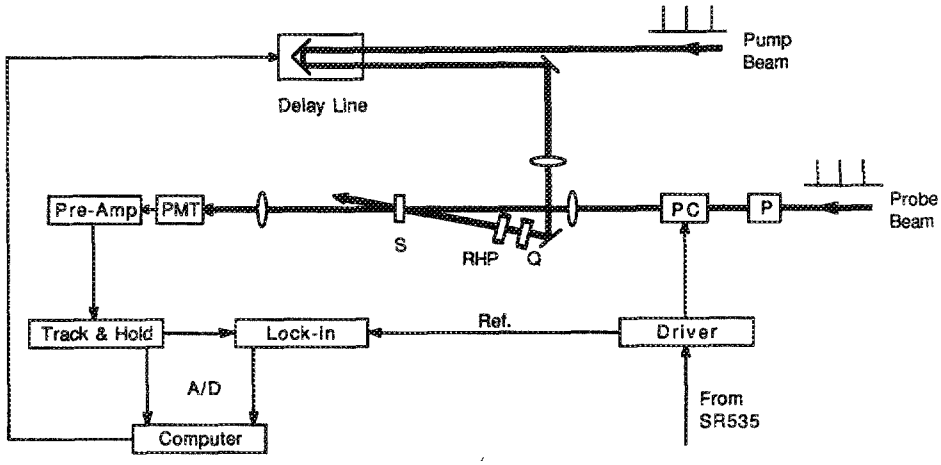

FIG. 3. Schematic of the detection system. Abbreviations: PC: Pockels cell, Q: quarter wave plate, RHP: rotating half-wave plate, S: sample cell, P: polarizer, PMT: photomultiplier.

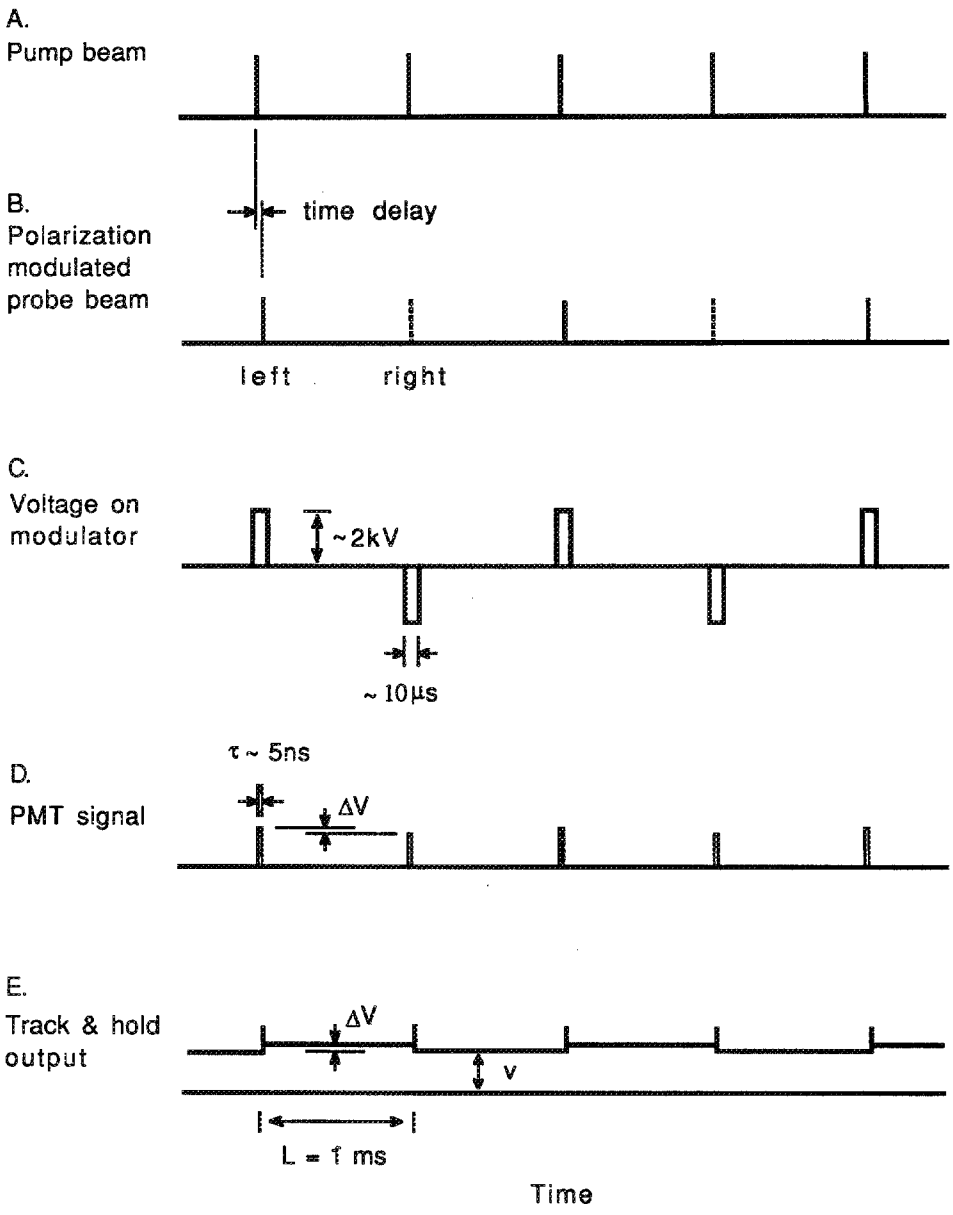

FIG. 4. Timing diagram for the detection system. The axes are exaggerated for demonstration purposes. A: pump beam pulse train, B: modulated probe pulse train, solid and dash lines represent left and right circularly polarized light, respectively. C: voltage applied on the electro-optic modulator. D: signal detected by PMT. E: signal with increased duty cycle from the track-hold circuit. The transient spikes which arise from on/off transition of the FET switch are inherent to the track-hold circuit. This high-frequency signal is easily removed by the lock-in amplifier and, thus, does not interfere with the CD measurement.

cond time-resolved circular dichroism experiment, and can be handled using a combination of phase sensitive detection and electronic track-and-hold circuits.

Phase sensitive detection can best be viewed in the frequency domain as a narrow bandpass filter with a bandwidth inversely proportional to the time constant. Referenced to a particular frequency, the output reflects the signal detected at this frequency, substantially suppressing noise signals at all other frequencies. In our particular case, the reference is the 500-Hz modulation rate of the electro-optic. The signal amplitude can be expressed by a Fourier series expansion:

$$f(t) = \frac{1}{2} a_0 + \sum_{n=1}^{\infty} a_n \cos(n\omega t + \phi) , \qquad (3)$$

where ω is the modulation frequency, and ϕ is the phase shift. By assuming rectangular pulses for simplicity, it is easy to show that the amplitude at the reference, a_1, is

$$a_1 = (2\Delta V/\pi)\sin(\pi\tau/2L) , \qquad (4)$$

where ΔV is the CD induced-voltage difference (on the order of mV), τ is the pulse duration (5 ns), and L is the time between pulses (1 ms). This implies an extraordinary small a_1 ($\approx$nV), virtually impossible to detect using a lock-in amplifier.

A solution to this problem is realized by processing the signal by a track-and-hold circuit (Stanford Research Systems model SR250), effectively increasing the duty cycle. The output from the track-and-hold, also shown in Fig. 4, is nearly a perfect square wave, resulting in $\tau \approx L$. In the limit of a perfect square wave, a_1 reaches a maximum, $2\Delta V/\pi$. At this point, the shape of the signal is identical to that detected in conventional CD spectrometers. The output of the track-and-hold circuit is sent to the lock-in amplifier (EG&G model 5209) for phase sensitive detection. Using this approach, the sensitivity of our experiment is substantially in-

creased. With a 3–10-s time constant, as demonstrated in the next section, we obtain a signal to noise ratio $> 10{:}1$. The remaining noise in our experiment results primarily from the fluctuation in laser pulse energies. We believe the track-and-hold and lock-in amplifier combination can be applied to other small signal measurements encountered in high-repetition picosecond experiment.

The output provided by the lock-in amplifier, S_{LIA}, is a root mean square voltage, or $(\sqrt{2}/2)a_1$. Combining with Eq. (4),

$$2(S_{\mathrm{LIA}}/\sqrt{2}) = 2\Delta V/\pi\,, \tag{5}$$

or

$$\Delta V = S_{\mathrm{LIA}} \times 2.221\,. \tag{6}$$

To relate this output signal to the circular dichroism of the sample, one notes that

$$\Delta A = (\Delta\epsilon)cl = \log(I_r/I_0) - \log(I_l/I_0) = \log(I_r) - \log(I_l) = \Delta\log(I)\,, \tag{7}$$

where c is the sample concentration, l is the cell path length, I_0 is the intensity of left and right circularly polarized light before entering the sample, and I_r and I_l are the corresponding intensities for left and right circularly polarized light after passing through the sample. Since the difference between I_r and I_l is very small, one can rewrite Eq. (7) as

$$\Delta A = \frac{\Delta\ln(I)}{2.303} \approx \frac{\Delta I}{2.303\times I} = \frac{\Delta V}{2.303\times V} = \frac{0.964\times S_{\mathrm{LIA}}}{V}\,, \tag{8}$$

where V is the amplitude of the DC component of the track-and-hold output.

In practice, both the output from the lock-in amplifier and the track-and-hold circuits are digitized by 16 bits A-D converters and processed by an on-line computer (IBM PC AT). These data are used to calculate the CD signal. When either the wavelength of the probe beam or the delay time between the pump and probe laser is changed, the high vol-

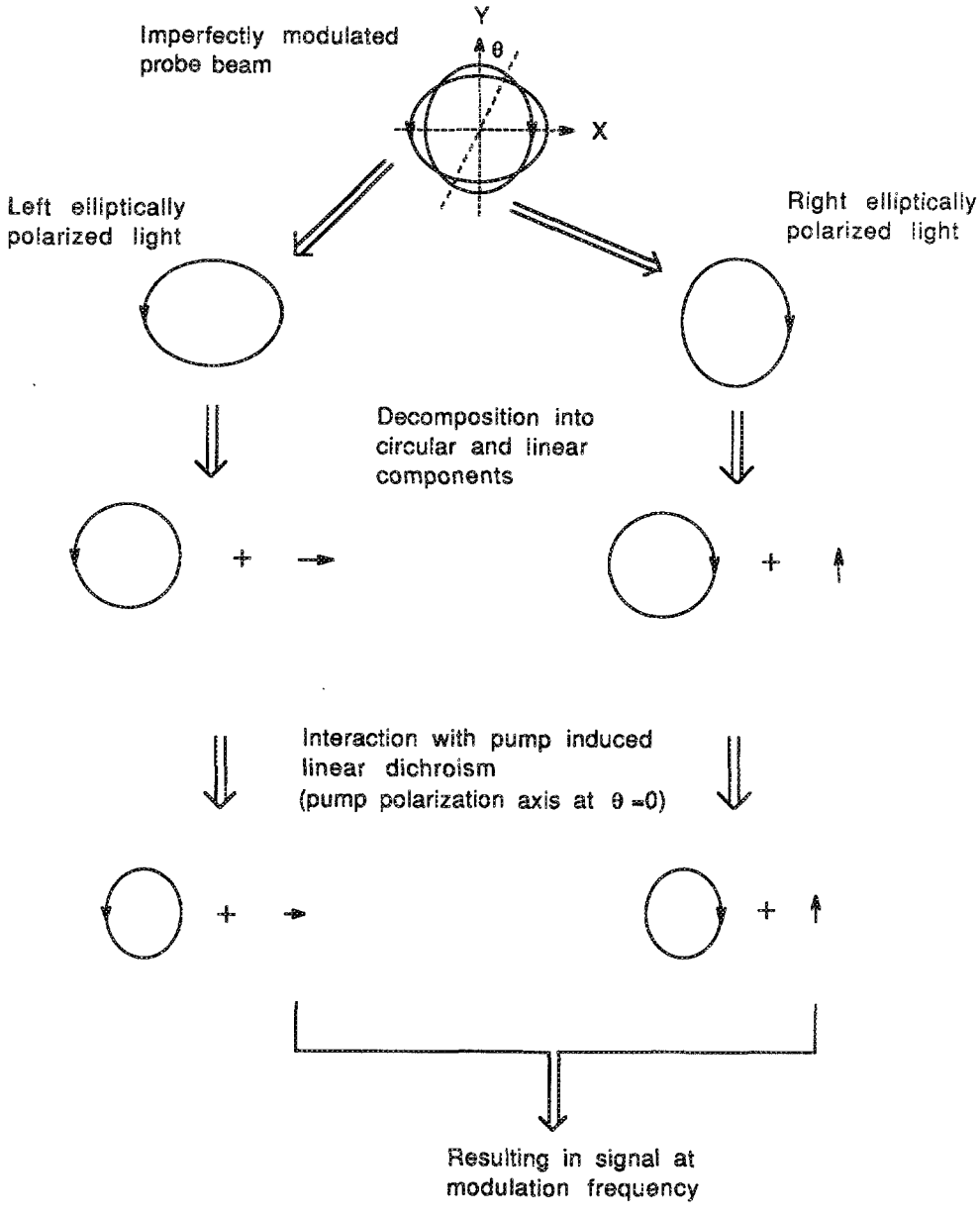

FIG. 5. Illustration of the effects of imperfectly modulated light and pump-induced linear dichroism. The left (or right) elliptically polarized light can be viewed as composed of a circular and a linear component. The two perpendicular linear components probe the linear dichroism induced by the pump beam and result in an additional signal at the modulation frequency. This signal is removed by spinning a half-wave plate in the excitation beam, see text and Appendix A.

tage applied to the photomultiplier is adjusted so that the peak voltages of the pulses remain roughly constant (2-V peak voltage after the signal is amplified by the preamplifier).

The pump beam is passed down an optical delay line (Velmex) with a maximum delay time of 10 ns. However, when two lasers are used, CD kinetics up to 60 ns can be obtained by cavity dumping the pump dye laser prior to the cavity dumping of the probe dye laser. The pump beam is focused onto the sample using a 40-cm focal length lens. The pump and probe beam are crossed at an angle $\approx 10°$.

One must take care to consider polarization effects which are induced by the pump laser. In principle, the linear dichroism does not interfere with the CD measurement. This can be seen as follows. Pure circularly polarized light can be viewed as composed of two linearly polarized components which are perpendicular to each other with a 90° phase difference. The linear dichroism of the sample would attenuate one of these linear components more than the other. However, the effect is identical for both left and right circularly polarized light, thus giving no signal at the modulation frequency. A complication arises when slightly elliptically polarized light with different sense (Fig. 5) is used to probe the sample. In practice this often happens for many reasons, i.e., misalignment of the Pockels cell, and strains in the lenses or cell window. As shown in Fig. 5, left (or right) elliptically polarized light possess both circular and linear components. The two perpendicualr linear components probe the linear dichroism induced by the pump beam and result in an additional signal at the modulation frequency. A mathematical treatment of the combined effects of linear dichroism and linear birefringence on the transient CD signal using a Jones matrix analysis[27] is outlined in Appendix A. It is important to note that such an analysis demonstrates that the pump-induced linear dichroism often dominates the measured signal.

Ideally, a depolarized beam is needed to prevent pump-induced linear dichroism or linear birefringence. In practice, complete depolarization of a laser beam is difficult to achieve. The contributions from both pump-induced linear birefringence and dichroism can also be eliminated by using a circularly polarized pump beam.[28] However, even with optimal alignment of the quarter-wave plate, we could not obtain a perfectly circularly polarized pump beam. Thus, contributions from the linear dichroism (rather than linear birefringence, see Appendix A) still spoiled our CD measurement. The Jones matrix analysis given in Appendix A demonstrates that the effects of pump-induced linear dichroism can be completely removed by spinning a half-wave plate in the pump beam. In our apparatus, the half-wave plate is spun at a frequency of 3.5 Hz, significantly different from the polarization modulation frequency. This causes a rotation of the polarization ellipse of the pump beam and consequently a modulation of the linear dichroism signal at twice the rotational frequency. This modulated signal can be easily distinguished and suppressed by the lock-in amplifier. Using a time constant of 3–10 s, much longer than the rotation cycle, the lock-in filters out the linear dichroism signal when referenced to the modulation frequency (500 Hz).

C. Electro-optic modulator for generating the circularly polarized probe beam

The electro-optic modulator used our picosecond time-resolved circular dichroism apparatus is a KD*P longitudinal Pockels cell (Quantum Technology model QK-8-1). Switching the polarity of the quarter-wave voltage applied to the Pockels cell causes the cell to alternate between $+1/4$ wave and $-1/4$ wave retardation, resulting in the desired modulation of the laser pulses. The quarter-wave voltage is a linear function of wavelength with 2.2 kV at 633 nm. The voltage on the Pockels cell and its timing is shown in Fig. 4. Pulsed rather than square or sine wave high voltage is applied for two reasons. First of all, the life time of the Pockels cell is dramatically increased using pulsed voltage. Second, and more importantly, square-wave switching of the high voltage at the reference frequency can couple a spurious modulation into the detected signal. Thus, for the reverse reasoning of increasing the Fourier component at the reference frequency for the CD signal, a reduced duty cycle is needed to eliminate the undesired coupling between phase sensitive detection and the polarization modulation system. In practice, the positive and negative high voltages are alternatively applied for only a few microseconds (see Fig. 4). The high-voltage polarity switching is done with a single adjustable positive high voltage power supply using the bridge circuit shown in Fig. 6. The solid state switches, K_1 and K_2, are alternatively triggered and turned on by a timing circuit illustrated in Fig. 7. This timing circuit is a simple digital device for counting-down and shaping a trigger pulse from the central laser timing control unit (the Stanford Research System model DG535 pulse delay generator). In addition to triggering K_1 and K_2, the circuit also provides a square wave at the modulation frequency to serve as the reference signal for the lock-in amplifier. Figure 8 shows the

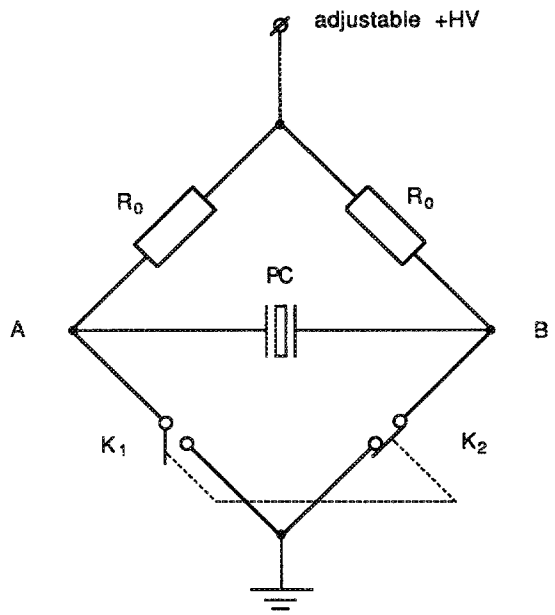

FIG. 6. Bridge circuit diagram for switching the polarity of the high voltage applied to the Pockels cell. PC: Pockels cell, R_0: 100 kΩ, 2 W. A schematic of the switch K_1 (or K_2) is given in Fig. 8.

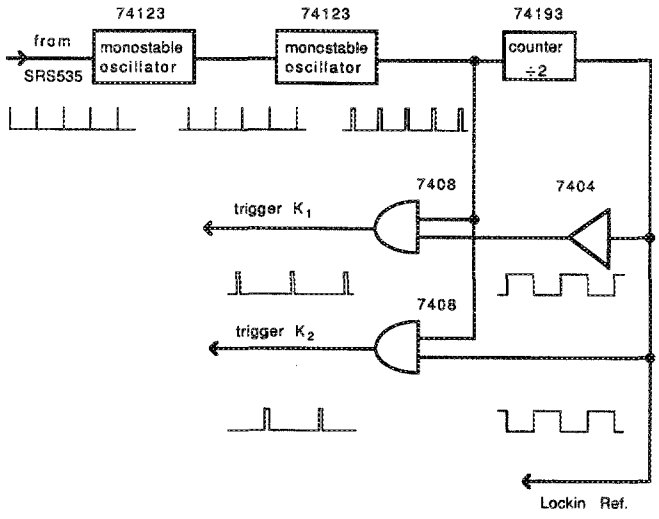

FIG. 7. Diagram for the timing circuit of the electro-optic modulator driver. Two monostable oscillators first delay and broaden the synchronous trigger pulses from the central laser timing control unit (SRS DG535). These pulses are then conditioned by simple TTL logic to produce the trigger pulses for K_1 and K_2 as well as a reference signal for the lock-in amplifier.

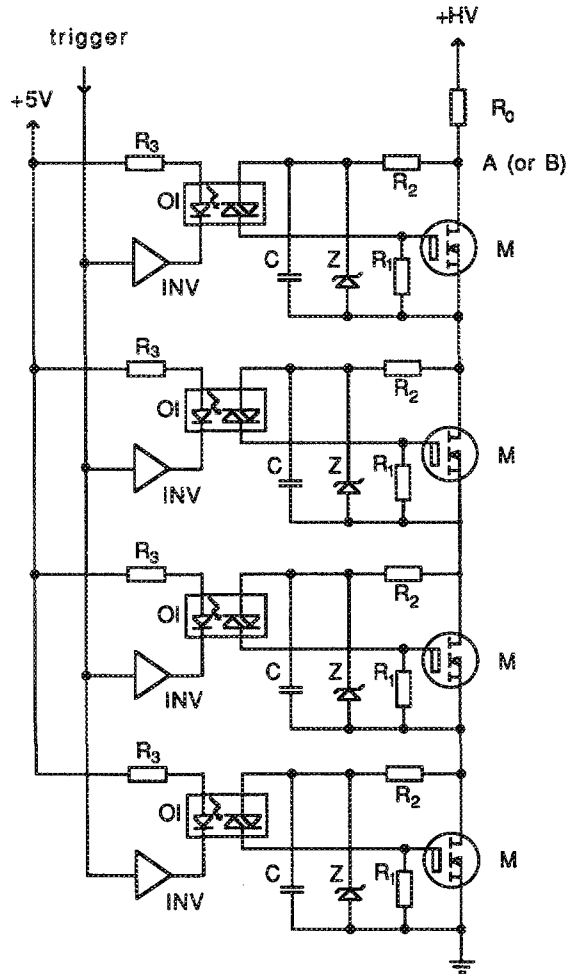

FIG. 8. Circuit diagram of the high-voltage switch K_1 (or K_2). This circuit is capable of switching 3.5 kV in less than a microsecond. It consists of four high-voltage power MOSFETs in series. The MOSFETs are simultaneously triggered by optically isolated triac drivers which are controlled by the timing circuit shown in Fig. 7. R_0: 100 kΩ, 2 W, R_1: 40 kΩ, R_2: 1 MΩ, R_3: 500 Ω, C: 510 pF, M: high-voltage power MOSFET, IXPT2N100A, OI: optical isolator, MOC3011, Z: 30–40 V, INV: inverter, 7404. Point A (or B) refers to the label in Fig. 6.

circuit diagram of the K_1 (K_2) switch. It consists of four high-voltage power MOSFETs in series, each MOSFET (IXYS, IXTP2N100A) can switch 1 kV within 100 ns. The MOSFETs are simultaneously triggered by optically isolated triac drivers (Motorola MOC3011). The switch is closed for several microseconds, this time is determined by the capacitance and resistance of C and R_1, respectively.

III. EXPERIMENTAL TIME-RESOLVED CIRCULAR DICHROISM STUDIES: PHOTOELIMINATION OF CO FROM CARBONMONOXYMYOGLOBIN

Our goal in developing picosecond time-resolved circular dichroism spectroscopy is to provide an experimental approach for studying ultrafast conformational motions of biomolecules. We are currently studying conformational changes following ligand photodetachment from heme proteins. The details of the photodissociation of ligated hemoglobin (Hb) and myoglobin (Mb) have received considerable attention in the last few years.[29] Questions concerning detailed kinetics of the photoinduced protein structural changes and the dynamical relationship between the inter- and intra-subunit conformational motions remain to be answered.

Picosecond time-resolved UV-visible absorption, resonance Raman, and IR spectroscopies have been applied to study these systems. This subject has been recently reviewed by Hochstrasser and coworkers.[6] Currently used experimental approaches are very sensitive to heme ligand binding but generally less sensitive to the protein structural changes. Since there is no measurable geminate recombination on the picosecond time scale between Mb and CO following photoelimination CO from MbCO, this system is the one of choice for monitoring the conformational motion following ligand detachment. Transient absorption studies show that a deoxy-like absorption spectrum appears within 350 fs of the photoexcitation of MbCO or Hb-CO. Closely resembling, but slightly different from equilibrium deoxymyoglobin, this transient persists for nanoseconds and is attributed to possible unrelaxed protein conformations. A recent optical study of heme properties[6] has detected no changes in the band shape of this transient absorption between tens of ps and a few ns. From this data, it has been concluded that the quaternary structure alterations occur later and that the intra-subunit structural changes that influence the rate of ligand rebinding are completed within tens of picoseconds. Time-resolved CD would be more informative concerning these structural changes.

There have been many steady-state CD studies of Mb and Hb derivatives.[30] These studies implied that by monitoring the time-dependent CD in the various absorption bands, different types of protein motions can be followed.[13] For example, CD in the far-UV range reflects the secondary structure of the protein and thus, does not change significantly upon ligand binding. CD in the aromatic region, particularly from 280–290 nm, is believed to be sensitive to the quaternary structure. For both Mb and Hb, large CD signals are observed in the Soret region $\lambda \approx 400$–450 nm. This absorption band is sensitive to ligand binding; thus, even if there

were not conformational change upon photodissociation, CD changes in this region would be observed upon ligand detachment due to the change in the electronic structure of the protein. However, it is believed that CD in this spectral range is also sensitive to the structural changes around the porphyrin ring. Theoretical calculations[31] indicate that the origin of the optical activity of the Soret band in Hb and Mb is due to coupled oscillator interactions between the porphyrin π-π^* transitions and the aromatic side-chains of the protein in the immediate vicinity of the heme. It has also been suggested that the CD of the Soret band could be used as a probe for tertiary and quarternary structures. In reality, a transient CD evolution different from that observed in a transient absorption study would provide definitive data on the dynamics of conformational relaxation in the protein.

Kliger and co-workers[20] have reported nanosecond time-resolved CD data for the photodissociation of CO from MbCO. Upon photolysis, the CD signal changes from that expected for MbCO to Mb within the time resolution of the experiment. No further change in signal is observed over the time scale of hundreds of nanoseconds. These data demonstrate the need to examine the time dependence of the CD signal with picosecond resolution.

In developing a time-resolved spectroscopic technique, it is important to verify that nontime-resolved data obtained on such an instrument is consistent with that obtained on a conventional spectrometer. In the case of circular dichroism, this means that if we collect data at a negative time delay (probe beam arrives at the sample before the pump), the CD spectrum obtained by scanning the probe dye laser should be identical to that obtained on a commercial instrument. In order to demonstrate that our experiment produces spectra which are equivalent to those from commercial devices, we collected the CD spectrum of deoxymyoglobin in the wavelength range from 550 to 600 nm (tuning over the dye curve of R6G). The CD spectrum in this region is due to the asymmetric environment of the heme. For comparison we have also collected the CD spectrum on a commercial apparatus (Cary 61). In Fig. 9, the two spectra are plotted. There is excellent agreement between the data obtained with the picosecond laser and that obtained with the traditional machine. This comparison clearly demonstrates that the polarization modulation technique and phase sensitive detection system used in the picosecond spectrometer accurately measures the amplitude of the CD signal.

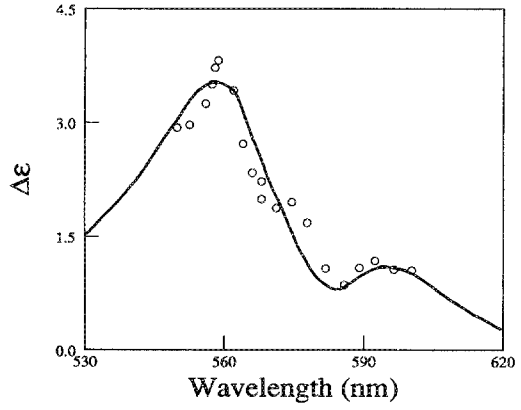

FIG. 9. Comparison of the steady-state CD spectrum of Mb from 550 to 600 nm recorded by our picosecond apparatus (points) with that obtained from a commercial Cary 61 CD spectrometer (solid line). The picosecond data is recorded at negative delay time (probe beam arriving at the sample before the pump).

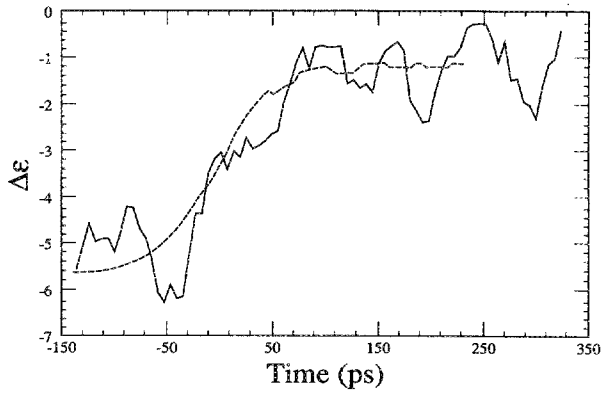

FIG. 10. CD value at 355 nm is plotted as a function of time with respect to excitation of MbCO by 532-nm light. The data show that the CD signal increases upon excitation. The dashed line is a scaling of the transient absorption data, providing a measure of the instrument response function.

We have carried out time-delay experiments probing the N-band (at $\lambda = 355$ nm) of Mb following photoelimination of CO from MbCO. The excitation pulse was at 532 nm; the time resolution of the experiment was limited by the pump pulse to ≈ 80 picoseconds. Pump and probe pulse energies of $60\,\mu$J/pulse and $< 1\,\mu$J/pulse were used, respectively. Horse met Mb was purchased from Sigma. The *p*H 7.0 phosphate buffer of MbCO was prepared as previously reported.[32] The Mb concentration was 0.9 mM, with a O.D. of 1.7 at 532 nm and > 4 at 355 nm. A 50 mℓ sample was circulated through the 2-mm flow cell under CO atmosphere. Previous CD studies show that MbCO has a negative CD signal at 355 nm.[20,33] On the other hand, Mb is characterized by $\Delta\epsilon \approx 0$ at this wavelength. In Fig. 9, the time resolved CD change is plotted. The dashed line is a transient absorption study (modulator off) of the MbCO photolysis, used to determine the instrument response function. The change in the CD signal from MbCO to Mb occurs on a time scale comparable to the response function.

It is important to note that the CD signals observed prior to photolysis (negative time) and for time delays greater than 300 picoseconds are within experimental error of the measured signal for pure samples of Mb and MbCO. At the pump energy used in this experiment, more than 90% of the MbCO molecules in the path of the probe beam are excited by the pump. Since there is no geminate recombination, we expect the signal at time delays > 100 ps to correspond to that due to essentially pure Mb. A complete study will be reported shortly.[33]

ACKNOWLEDGMENTS

This work is supported by the Presidential Young Investigators Program administered by the National Science

Foundation. We are indebted to Joseph P. Taulane for many stimulating discussions. We thank Professor Michael Fayer for helpful discussions on laser design and Professor Dana Dlott for a preprint of his article describing a power MOSFET design for electro-optic laser cavity dumping. J.D.S. is a NSF Presidential Young Investigator (1985–1990) and an Alfred P. Sloan Fellow (1988–1990).

APPENDIX A: MODELING OF THE EXPERIMENTAL APPARATUS

In this section, we present a Jones matrix analysis[27] of our experimental apparatus. These calculations show that the signal detected by our picosecond time-resolved circular dichroism spectrometer is free of (1) the effects of the circular birefringence of the sample, and (2) pump-induced linear dichroism and linear birefringence. Assuming that the light is propagating in the z direction, the polarization of the light in the x,y plane can be described by a column matrix

$$\mathsf{J} = \begin{bmatrix} E_x e^{i\phi_x} \\ E_y e^{i\phi_y} \end{bmatrix}, \tag{A1}$$

where E_x, E_y are the amplitudes of the x,y components of the light, and ϕ_x, ϕ_y are the corresponding phase shifts. We can use this representation to describe left circularly ($E_x = E_y$, $\phi_x = \pi/2$, $\phi_y = 0$), and right circularly ($E_x = E_y$, $\phi_x = -\pi/2$, $\phi_y = 0$) polarized light. For the following calculations, the x axis is defined by the polarization of the pump beam. The intensity of the light is given by $E^2 = E_x^2 + E_y^2$. The effect of an optical element on the probe light is described by the product of the above column matrix by the appropriate Jones matrix for the optical process.

In modeling the experimental apparatus, we simply need to write down the matrix representation for the various optical components, resulting in a mathematical expression for how the apparatus (optics and sample) interacts with the pump and probe light. Comparing the calculated results for left and right circularly polarized light, we can evaluate the detected signal. In this manner, the effects of linear birefringence of the optics as well as pump-induced linear birefringence and linear dichroism on the observed signal can be evaluated.

The linear birefringence of the sample cell, lenses, and Pockels can be expressed in terms of the following matrix, M_{lb}.

$$\mathsf{M}_{\mathrm{lb}} = \begin{bmatrix} \cos^2\theta e^{ib} + \sin^2\theta e^{-ib} & i\sin 2\theta \sin b \\ i\sin 2\theta \sin b & \cos^2\theta e^{-ib} + \sin^2\theta e^{ib} \end{bmatrix}. \tag{A2}$$

In this matrix, θ is the angle of the fast axis of the optic with respect to the pump polarization and $2b$ is the retardation. In addition, we need to consider the pump-induced linear birefringence and linear dichroism in the sample. These effects can be expressed by the following matrix:

$$\mathsf{M}'_{\mathrm{LB,LD}} = \begin{bmatrix} me^{-i\rho} & 0 \\ 0 & m'e^{i\rho} \end{bmatrix}. \tag{A3}$$

In the above matrix, m^2 and m'^2 are the transmissions of the two perpendicular linear polarization axes. The angle, 2ρ is the retardation caused by the pump-induced linear birefringence. The axes of the two components of the probe light are defined by the polarization axis of the pump beam.

Circular dichroism of the sample can be represented by the following Jones matrix:

$$\mathsf{M}_{\mathrm{CD}} = \frac{1}{2}\begin{bmatrix} k+k' & -i(k-k') \\ i(k-k') & k+k' \end{bmatrix}, \tag{A4}$$

where k'^2 and k^2 are the transmittance of left and right circularly polarized light.

The Jones matrix for the circular birefringence of the sample is expressed by

$$\mathsf{M}_{\mathrm{CB}} = \begin{bmatrix} \cos\omega & -\sin\omega \\ \sin\omega & \cos\omega \end{bmatrix}, \tag{A5}$$

where $\omega = \pi(n_R - n_L)/\lambda$, l is the sample path length and λ is the wavelength of the incident light.

We want to evaluate the contribution of each of these effects to the observed experimental signal. In our apparatus, we measure the ratio of the output of the lock-in amplifier, S_{LIA} to the DC component of the output of the track-and-hold circuit, V:

$$\Delta A = 0.964\, S_{\mathrm{LIA}}/V. \tag{A6}$$

The output of the lock-in amplifier is related to the difference in the intensities of the transmitted left and right circularly polarized light beams, $E_L^2 - E_R^2$ and the DC component of the track-and-hold output is simply related to the sum of these two intensities $E_L^2 + E_R^2$. In the perfect case of no complications from any polarization artifacts, the equivalent matrix representation of this ratio gives the following detected signal:

$$(E_L^2 - E_R^2)/(E_L^2 + E_R^2) = (k'^2 - k^2)/(k'^2 + k^2). \tag{A7}$$

The signal is simply proportional to the circular dichroism of the sample.

It is important to stress that our measurment is free from the influence of circular birefringence. This can be seen from the following analysis. The matrices for circular dichroism and circular birefringence commute, the expected signal is still given by Eq. (A7) for both (1) $\mathsf{M}_{\mathrm{CD}} \times \mathsf{M}_{\mathrm{CB}} \times \mathsf{J}_{\mathrm{left,right}}$, and (2) $\mathsf{M}_{\mathrm{CB}} \times \mathsf{M}_{\mathrm{CD}} \times \mathsf{J}_{\mathrm{left,right}}$, clearly showing that the signal is independent of any circular birefringence of the sample.

We now turn to examining the combined effects of linear birefringence and pump-induced linear birefringence, and pump-induced linear dichroism on this signal. Unfortunately, the matrix presentation for CD does not commute with the matrix for pump-induced linear birefringence and dichroism, $\mathsf{M}'_{\mathrm{LB,LD}}$. A rigorous evaluation is possible using the Jones N-matrix[27] method, and such a calculation will be published shortly.[34] However, for demonstration purposes, we will look at the two limiting cases: (1) $\mathsf{M}'_{\mathrm{LB,LD}} \times \mathsf{M}_{\mathrm{CD}} \times \mathsf{M}_{\mathrm{LB}} \times \mathsf{J}_{\mathrm{left,right}}$, and (2) $\mathsf{M}_{\mathrm{CD}} \times \mathsf{M}'_{\mathrm{LB,LD}} \times \mathsf{M}_{\mathrm{LB}} \times \mathsf{J}_{\mathrm{left,right}}$, evaluating in each case the effect of these additional polarization properties on the experimentally measured signal.

For case one, the signal measured is given by

$$\frac{E_L^2 - E_R^2}{E_L^2 + E_R^2} = \frac{k'^2 - k^2}{k^2 + k'^2}\cos 2b + 2\frac{[(m'^2 - m^2)/(m^2 + m'^2)]kk' \sin 2\theta \sin 2b}{(k'^2 + k^2)}. \tag{A8}$$

Because the magnitude of the linear dichroism signal is generally larger than the CD signal ($m'^2 - m^2 \gg k'^2 - k^2$), the second term in the above expression often dominates. Even a quarter-wave plate or a pseudodepolarized in the pump beam cannot, in practice, completely remove this term. As described in the previous section, in our experimental apparatus, there is a rotating half-wave plate in the excitation beam. This, in effect, causes the value of θ to vary in time. Since the lock-in time constant is significantly longer than the rotation time of the wave plate, the observed signal corresponds to an averaging of the above quantity over $\theta = 0$ to $\theta = 2\pi$. This simplifies the above expression to give the following:

$$\frac{E_L^2 - E_R^2}{E_L^2 + E_R^2} = \frac{k'^2 - k^2}{k^2 + k'^2}\cos 2b. \tag{A9}$$

Thus, in this limit, the pumped-induced linear dichroism and linear birefringence have no effect on the observed signal; the signal measured is reduced from the true value of the CD of the sample by the linear birefringence of the cell and optics. This is the same for all commercial CD spectrometers as well. The linear birefringence of the optics and sample can be determined. In our case, we find that $b < 2°$. In general, this quantity is time independent and, thus, has no effect on the observed kinetics. Furthermore, if we have considerable linear birefringence, i.e., $b = 5°$, then $\cos(2b) = 1 - 2b^2 \approx 0.985$, the signal is only reduced to 98% of its true value, well within the S/N ratio for the current apparatus.

For case two, the mathematical form of the measured signal is more complicated. The order of matrix multiplication is now such that the contribution of pump-induced linear birefringence and dichroism to the experimental signal is overestimated. In this case, we obtain

$$\frac{E_L^2 - E_R^2}{E_L^2 + E_R^2} = \frac{2\,\mathrm{mm}'}{m^2 + m'^2}\frac{k'^2 - k^2}{k^2 + k'^2}(\cos 2\rho \cos 2b + \sin 2\rho \sin 2b \cos 2\theta) + \frac{m^2 - m'^2}{m^2 + m'^2}\sin 2\theta \sin 2b. \tag{A10}$$

Once again, averaging over the rotation of θ achieved by rotating the half-wave plate in the excitation beam:

$$\frac{E_L^2 - E_R^2}{E_L^2 + E_R^2} = \frac{2\,\mathrm{mm}'}{m^2 + m'^2}\frac{k'^2 - k^2}{k^2 + k'^2}(\cos 2\rho \cos 2b). \tag{A11}$$

The above expression shows that both pump-induced linear birefringence and dichroism reduce the signal from the true CD value of the sample. However, as described in Sec. II, in addition to the rotating half wave-plate, we use a quarter-wave plate to circularly polarize the pump. This gives us an experimental way of achieving $m \approx m'$ and $\rho \approx 0$, thus eliminating the effect of pump-induced linear birefringence and dichroism. Thus, as in the previous calculation, the signal measured is slightly reduced from the absolute value of CD by the linear birefringence of the cell and optics ($\cos 2b$) but the effects of pump-induced linear polarization are eliminated.

[1]C. R. Cantor and P. R. Schimmel, *Biophysical Chemistry* (Freeman and Co., New York, 1980).
[2]G. A. Petsko and D. Ringe, Ann. Rev. Biophys. Bioeng. **13**, 331 (1984).
[3]B. P. Maliwal and J. R. Lakowicz, Biophys. Chem. **19**, 337 (1984); A. J. Cross and G. R. Fleming, J. Biophys. **50**, 507 (1986); J. W. Jaroszewski, K. Schaumburg, and H. Kofod, Eds., *NMR Spectroscopy in Drug Research* (Munksgaard, Copenhagen, 1988); O. Jardetzky and G. C. K. Roberts, *NMR in Molecular Biology* (Academic, Orlando, 1981).
[4]J. M. Beechem and L. Brand, Ann. Rev. Biochem. **54**, 43 (1985).
[5]M. A. Kahlow, W. Jarzeba, T. P. DuBruil, and P. F. Barbara, Rev. Sci. Instrum. **59**, 1098 (1988).
[6]R. M. Hochstrasser and C. K. Johnson, in *Ultrashort Light Pulses and Applications*, edited by W. Kaiser (Springer, New York, 1988).
[7]P. M. Bayley and M. Anson, Biopolymers **13**, 401 (1974).
[8]F. A. Ferrone, J. J. Hopfield, and S. E. Schnatterly, Rev. Sci. Instrum. **45**, 1392 (1974).
[9]I. Tabushi, K. Kamamura, and T. Nishiya, J. Amer. Chem. Soc. **101**, 2785 (1979).
[10]D. A. McQuarrie, *Statistical Mechanics* (Harper and Row, New York, 1976).
[11]S. F. Mason, *Molecular Optical Activity and the Chiral Discriminations* (Cambridge University Press, Cambridge, MA, 1982).
[12]For a review see J. A. Schellman, Chem. Rev. **75**, 323 (1975).
[13]S. Beychok, I. Tyuma, R. E. Benesch, and R. Benesch, J. Biol. Chem. **242**, 2460 (1967); S. R. Simon and C. R. Cantor, Proc. Natl. Acad. Sci. USA **63**, 205 (1969).
[14]See G. Bruhat, *Traite de Polarimetrie* (Editions de la Revue d'Optique, Paris, 1930).
[15]L. Velluz, M. Legrand, and M. Grosjean, *Optical Circular Dichroism* (Verlag Chemie, New York, 1965).
[16]A. F. Drake, J. Phys. E **30**, 170 (1986).
[17]D. S. Kliger and J. W. Lewis, Rev. Chem. Intermed. **8**, 367 (1987).
[18]J. W. Lewis, R. F. Tilton, C. M. Einterz, S. J. Midler, I. D. Kuntz, and D. S. Kliger, J. Phys. Chem. **89**, 289 (1985).
[19]C. M. Einterz, J. W. Lewis, S. J. Milder, and D. S. Kliger, J. Phys. Chem. **89**, 3845 (1985).
[20]S. J. Milder, S. C. Bjorling, I. D. Kuntz, and D. S. Kliger, Biophys. J. **53**, 659 (1988).
[21]C. V. Shank and E. P. Ippen, Appl. Phys. Lett. **26**, 62 (1975).
[22]D. Waldeck, A. J. Cross, D. B. McDonald, and G. R. Fleming, J. Chem. Phys. **74**, 15 (1981).
[23]X. Xie and J. D. Simon, Opt. Comm. **69**, 323 (1988).
[24]J. C. Postlewaite, J. B. Miers, C. C. Reiner, and D. D. Dlott, IEEE J. Quant. Electron. **QE-24**, 411 (1988).
[25]T. Sizer, J. D. Kafka, I. N. Duling, C. W. Gabel, and G. A. Mourou, IEEE J. Quant. Electron. **QE-19**, 506 (1983).
[26]D. B. McDonald and C. D. Jonah, Rev. Sci. Instrum. **55**, 1166 (1984).
[27]R. C. Jones, J. Opt. Soc. Am. **31**, 488 (1941); **31**, 493 (1941); **31**, 500 (1941); **32**, 486 (1942); **37**, 107 (1947); **37**, 110 (1947); **38**, 671 (1948).

[28]Using a circularly polarized pump light could result in a pump-induced circular dichroism. However, in our case, excitation by both left and right

circularly polarized light results in identical signals, demonstrating that this effect is negligible.
[29]C. Ho, Ed., *Hemoglobin and Oxygen Binding* (Elsevier Biomedical, New York, 1985), p. 371; J. M. Friedman, D. L. Rousseau, and M. R. Ondrias, Ann. Rev. Phys. Chem. **33**, 471 (1982); R. E. Dickerson and I. Geis, *Hemoglobin* (Benjamin Cummings, New York, 1983).
[30]Y. Sugita, M. Nagai, and Y. Yoneyama, J. Biol. Chem. **246**, 383 (1971); R. Woody in *Biochemical and Clinical Aspects of Hemoglobin Abnormalities* (Academic, New York, 1978).
[31]M-C. Hsu and R. W. Woody, J. Amer. Chem. Soc. **91**, 3679 (1969); M-C. Hsu and R. W. Woody, J. Amer. Chem. Soc. **93**, 3515 (1971).
[32]T. Samejima and J. T. Yang, J. Mol. Biol. **8**, 863 (1964).
[33]X. Xie and J. D. Simon (unpublished).
[34]X. Xie and J. D. Simon (unpublished).